Biosensors and Bioelectronics 128 (2019) 1–8

Contents lists available at ScienceDirect

Biosensors and Bioelectronics

journal homepage: www.elsevier.com/locate/bios

# An electrochemical sensor for attomolar determination of mercury(II) using DNA/poly-L-methionine-gold nanoparticles/pencil graphite electrode

Hamid Reza Akbari Hasanjani, Kobra Zarei*

*School of Chemistry, Damghan University, Damghan, Iran*

ARTICLE INFO

*Keywords:*
Poly L-methionine
Gold nanoparticles
Deoxyribonucleic acid (DNA)
Mercury(II)
Square wave anodic stripping voltammetry

ABSTRACT

The present work describes an ultrasensitive electrochemical sensor for determination of mercury(II) using deoxyribonucleic acid/poly-L-methionine-gold nanoparticles/pencil graphite electrode (DNA/PMET-AuNPs/PGE). To fabricate this biosensor, L-methionine (L-MET) was electropolymerized on the PGE surface followed by simultaneous electrochemical entrapment of AuNPs. Next, DNA was immobilized on the PMET-AuNPs/PGE by applying a 0.5 V potential. The surface area of modified and unmodified electrodes was determined by chronocoulometric technique. $Hg^{2+}$ was detected in the linear dynamic range of 0.1 aM to 0.1 nM, and the detection limit was determined as 0.004 aM using square wave anodic stripping voltammetry (SWASV) under optimized conditions. The DNA/PMET-AuNPs/PGE demonstrated good selectivity toward $Hg^{2+}$ against other metal ions such as $V^{4+}$, $Pb^{2+}$, $Cr^{3+}$, $Cd^{2+}$, $Cu^{2+}$, $Zn^{2+}$, $Sn^{2+}$, $In^{3+}$, $Ge^{4+}$, and $Fe^{3+}$. Real samples studies were carried out in sea water and fish samples.

## 1. Introduction

Mercury is a heavy metal with high toxicity even at low concentrations. Despite the importance of mercury in the industry, the environmental pollution caused by this metal is a very major problem (Duffus and Worth, 2006). Mercury using causes abnormal functions of the brain, kidney, liver, eyes, and bones upon accumulation in the body (Aragay and Merkoçi, 2012; Ramesh and Radhakrishnan, 2011). The toxicity of mercury at low levels necessitates analyzing it in water and other samples (Cui et al., 2015).

There are several methods for detecting trace amounts of $Hg^{2+}$. Conventional $Hg^{2+}$ detection methods include flame atomic absorption spectrometry (FAAS) (Ghaedi et al., 2007), graphite furnace atomic absorption spectrometry (GFAAS) (Nowka et al., 1999), inductively coupled plasma mass spectrometry (ICP-MS) (Gómez-Ariza et al., 2005), inductively coupled plasma atomic emission spectrometry (ICP-AES) (Zhu and Alexandratos, 2007), and UV–Vis spectroscopy (Yin et al., 2012). However, these methods do not meet the demands for a portable, easy-to-use, quick and cheap analysis. Pay attention thus that the US Environmental Protection Agency (EPA) limit of $Hg^{2+}$ for drinkable water is 10 nM, which is much less than the detection of most available assays. In this case, electrochemical analysis of heavy metals is an alternative to conventional methods and also it has a high sensitivity (H. Wang et al., 2016). Electrochemistry offers unique application possibilities in the field of heavy metal analysis because of the compact, simple, and portable instrumentation, low cost, less complex of instrumentation, shorter measuring time, electrode miniaturization, and easy electrode modification (Locatelli and Melucci, 2013; Nejdl et al., 2013, 2014). Various electrochemical sensors for determination of $Hg^{2+}$ ion have been reported including siliceous mesocellular foam (Bojdi et al., 2016), Schiff-base ligand (Nourifard et al., 2015), and ion imprinted polymer (Shirzadmehr et al., 2015). Biomaterials such as enzymes, amino acids, peptides, cells, and nucleic acids that can produce very selective and specific interactions, are the most important candidates for electrochemical detection of heavy metal ions (Cui et al., 2015).

The modification of polymeric species by coating onto the electrode surfaces (especially using the electropolymerization technique) gives a wide flexibility because they contain functional groups that can provide excellent high surface coverage using thick multilayer coating. L-methionine can be directly electropolymerized as a porous and conductive polymer, onto electrode from monomers (Ojani et al., 2013; Reza Ojani et al., 2014; Venkataprasad et al., 2018). Also, this amino acid is highly useful for immobilization of nucleic acids because of the presence of carboxyl groups (Abdul Rashid and Yusof, 2017). In this regard, $–NH_2$ and –COOH groups of amino acids play important role in the electropolymerization process on the electrode surface (Zhang et al., 2013). In order to enhance sensitivity and amplify the electrochemical response,

* Corresponding author.
*E-mail address:* zarei@du.ac.ir (K. Zarei).

https://doi.org/10.1016/j.bios.2018.12.039
Received 24 September 2018; Received in revised form 19 December 2018; Accepted 19 December 2018
Available online 27 December 2018
0956-5663/ 

nanoparticles (NPs) are used as the Supporting material in the preparation of modified electrode (Zhu et al., 2014). The presence of NPs on the electrode surface enables fast electron transfer kinetics, increases the electroactive surface area, and reduces over-potential. Gold nanoparticles (AuNPs) with unique properties such as high conductivity, good biocompatibility, and large specific surface area are very attractive materials for sensors and biosensors. Many studies have used AuNPs modified electrodes for voltammetric sensing (Azadmehr and Zarei, 2018; Bernalte et al., 2012; Zarei and Khodadadi, 2017). Gold is an appropriate matrix for the electrochemical determination of $Hg^{2+}$ because of its high affinity toward $Hg^2$ that can increase preconcentration effect (N. Wang et al., 2016). Gold nanoparticles can bind to the surface of many polymers through covalent bonding to functional groups such as CN, $NH_2$, and SH (Reza Ojani et al., 2014). Thus, it seems L-methionine that contains $NH_2$ group can form chemical bond with gold nanoparticles.

Deoxyribonucleic acid (DNA) can be used for the expansion of heavy metals sensors, such as mercury, cadmium, and leads sensors, since they can form complexes with the selected nucleic acid bases. DNA is the main biomolecule that has recently attracted considerable attention because of its ability to bind small ligand molecules with high affinity and specificity. Small molecules interact with DNA in two well-characterized binding modes: covalent mod and reversible non-covalent binding mode (electrostatic, groove binding, and intercalation). The investigations of DNA biosensors are currently under intense review because of their attractive properties such as sensitivity, selectivity, simplicity, rapidity, and low cost. The interactions of metal ions with DNA have been investigated extensively and are known to alter the DNA's structure and function. DNA has four different principal binding sites for metal ions: the negatively charged phosphate backbone, the ribose hydroxyls, the base ring nitrogen's, and the exocyclic base keto groups (Anastassopoulou, 2003). In ds-DNA, such coordination tends to cause changes in the structure of the double helix. For example, it has been found that $Hg^{2+}$ can bring two thymine (T) bases in the two strands together to form an $Hg^{2+}$ connected metal–base pair T–$Hg^{2+}$–T, which deforms the classic Watson–Crick double helix structure (Zhang and Guo, 2012). The changes are dependent on the sequence of base pairs but tend to form a hairpin structure. Interference analysis with other common metal ions suggests that T-T interactions are specific to $Hg^{2+}$. Therefore, the sensor and biosensors based on DNA structure changes have a high selectivity and sensitivity. Although DNA biosensors for measuring of mercury have been reported (Tang et al., 2012; Wu et al., 2010; Zhang et al., 2015), there is no report on biosensor design based on DNA/PMET-AuNPs/PGE.

In the present study, we have modified a pencil graphite electrode (PGE) by DNA/poly L-methionine-gold nanoparticles (DNA/PMET-AuNPs) for the detection of $Hg^{2+}$ in the aqueous medium by the square wave anodic stripping voltammetry (SWASV). Application of very sensitive SWASV method for determination of $Hg^{2+}$ can help to increase the sensitivity. This sensor showed a very low detection limit with respect to the high interaction of $Hg^{2+}$ with DNA and poly L-methionine and also due to the AuNPs effect. Furthermore, the analytical performance of the DNA/PMET-AuNPs/PGE, such as linear range, reproducibility, and stability were investigated and it was used as a useful electrode for electrochemical determination of $Hg^{2+}$ in environmental samples.

## 2. Experimental

### 2.1. Reagents and materials

Deoxyribonucleic acid sodium salt from salmon testes (DNA with CAS number: 438545-06-3) was purchased from Sigma-Aldrich. L-methionine, mercury(II) nitrate, and gold(III) chloride trihydrate were procured from the Merck company. The stock solution (100.0 ppm DNA) was prepared using Tris-HCl buffer solution (pH 7.0) and preserved in the freezer. Diluted solutions of the DNA were prepared using Tris-HCl buffer solution. L-methionine was dissolved in phosphate buffer solutions (PBS) with pH 7.0 (0.05 M), prepared using 0.05 M $K_2HPO_4$ and $KH_2PO_4$ solutions.

### 2.2. Apparatus

The voltammetric measurements were done with a Dropsens portable bipotentiostat/galvanostat μSTAT 400 instrument. Autolab potentiostat/galvanostat-12 electrochemical system was applied for electrochemical impedance spectroscopic (EIS) measurements. The Dropview 8400 and FRA 4.9 softwares were applied for voltammetric and EIS tests, respectively. The utilized three-electrode system was composed of a DNA/PMET-AuNPs/PGE as a working electrode, a platinum wire as the counter electrode, and an Ag/AgCl/KCl (saturated) as the reference electrode. The pencil graphite was accessible as pencil lead purchased from Owner Co. (Korea, type HB, 0.5 mm diameter, surface area 0.159 $cm^2$). A mechanical pencil was applied as a holder for the graphite leads. The electrical contact with the lead was obtained by soldering a metal wire to the metal part of the holder. Spectra were recorded and stored using a Perkin Elmer Lambda 25 spectrophotometer with a PC using a 1-cm path length quartz cell. The Metrohm pH meter (Model 827) was applied to control the pH value of the solutions.

EIS was carried out in the presence of 5.0 mM $K_3[Fe(CN)_6]/K_4[Fe(CN)_6]$ in 0.1 M KCl as a redox probe in the frequency range of 0.1 Hz to 100 kHz, polarization potential of 0.15 V, and amplitude of 5 mV. The surface morphology of the modified electrode was characterized using field emission scanning electron microscopy and energy dispersive X-ray spectroscopy (FESEM-EDX) (model MIRA3TESCAN-XMU). Atomic force microscopy (AFM) was performed by a DME microscope with 95-50 E probe model.

### 2.3. Electrode modification

#### 2.3.1. Modification of the poly L-methionine-gold nanoparticle/PGE (PMET-AuNPs/PGE)

The electrode was initially cleaned in ultrapure water two times and then in 50:50 (v/v) ethanol/water solution. The electrode modification of PMET-AuNPs on PGE was performed using cyclic voltammetric (CV) technique in the potential range of -0.6 V to 2 V with a scan rate of 100 mV $s^{-1}$ during 6 cycles and in 8.0 mM L-methionine (L-MET) and 48.6 μM $HAuCl_4$ with PBS (pH 7.0).

#### 2.3.2. Immobilization of DNA on the PMET-AuNPs /PGE

After modification of the electrode by PMET and gold nanoparticles (PMET-AuNPs /PGE), the DNA was immobilized on the PMET-AuNPs /PGE using a potential of +0.5 V for 200 s from a stirred solution containing 10.0 ppm DNA in a Tris-HCl buffer solution (pH 7.0). In this way, DNA/PMET-AuNPs/PGE was prepared and dried at the room temperature and applied to determine $Hg^{2+}$.

### 2.4. Preparation of real samples

The method was used to analyze $Hg^{2+}$ in three water samples collected from the Caspian Sea (Gilan, Iran). Before using the samples, they were mixed and filtered (Whatman filter paper) through a membrane with a diameter of 0.45 μm.

The Caspian white fishes were collected from the Caspian Sea in Gilan province of Iran. The samples were placed in clean plastic bags and stored on ice in an ice chest. They were then transported to the laboratory and kept in a freezer at −20 °C prior to preparation for chemical analysis. A portion of the muscles was taken out quickly and was dried in an oven at 70 °C for 48 h. After grinding the dry tissue, 0.5 g of the sample was digested with 5 mL of concentrated $HNO_3$ for 4 h at 100 °C. The resulted mixture was filtered and transferred into

100 mL flask and then diluted with double distillated water up to 100 mL. The $Hg^{2+}$ content of the sample was analyzed by the proposed method.

### 2.5. Procedure

The sample solution containing $Hg^{2+}$ in acetic acid (pH 3.0) was transported to the voltammetric cell and the deposition potential 0 V was applied to the working electrode for 250 s while stirring the solution. Following the deposition period, the stirrer was halted and the square wave voltammogram was recorded from −0.5 to +0.6 V (vs. Ag/AgCl/KCl (saturated)) with a frequency of 20 Hz and a step potential of 5 mV. A blank solution without $Hg^{2+}$ was applied to obtain the blank peak current.

## 3. Results and discussion

### 3.1. Electropolymerization of L–methionine, and fabrication of PMET-AuNPs/PGE and DNA/PMET-AuNPs /PGE

The electropolymerization of L-MET using the cyclic voltammetry (CV) in the potential range of -0.6 to 2 V has been reported (Ojani et al., 2013). Also, the electrochemical entrapment of AuNPs has been performed with CV in the same potential range during 5 cycles (Rezaei et al., 2015). Fig. S1 shows CVs of 8.0 mM L-methionine and 48.6 μM $HAuCl_4$ in 0.05 M PBS (pH 7.0) solution on the PGE in the potential range of -0.6 to 2 V. As can be seen, in the initial potential sweep, an irreversible oxidation peak appears at 1.50 V. However, after the second cycle scanning, the peak potential shifted to the cathodic direction, while the peak current decreased. The variations in the peak potential, displays simpler oxidation in the further cycles. The possible reason for variations in the peak potential was due to the formation of polymer membrane and its connection to the electrode surface and also the effect of the formation of AuNPs on the electrode surface. The peak current slowly changes using further cycles. Scheme 1 illustrates the design of the DNA/PMET-AuNPs/PGE electrochemical sensor and the steps involved in the $Hg^{2+}$ electrochemical determination based on signal amplification of PMET-AuNPs and specific combination between $Hg^{2+}$ and DNA especially, T bases of DNA, to form stable T- $Hg^{2+}$-T linkage (Zhang and Guo, 2012). As can be seen, L-methionine initially is oxidized to form free radicals at the surface of the electrode that can attach to the surface of PGE and the formed product reacts with another L-Met by the elimination of water molecule to form a conductive polymer film on the electrode surface (Ojani et al., 2013; Venkataprasad et al., 2018). Simultaneously, AuNPs are simply formed during cyclic voltammetry scans and the progress of electropolymerization and possibility bind to the polymer through amide bonds (Rafiee et al., 2015). Since metal nano particles at the electrode surface can be fragile in the absence of a stabilizing material, the electrode should be modified with stabilizing material such as polymers (Reza Ojani et al., 2014). The porous structure of conductive polymers allows the AuNPs to disperse into the polymer matrix and generate additional active sites (Reza Ojani et al., 2014). Finally, DNA is immobilized on the fabricated PMET-AuNPs/PGE by applying a constant potential. DNA is able to use their bases (adenine, thymine, guanine, and cytosine) to be adsorbed onto the AuNPs surfaces via coordination interaction between bases and AuNPs (Zuo et al., 2010). Two major bonding factors govern this interaction: the anchoring, either of the Au-N or Au-O type, and the nonconventional N-H…Au hydrogen bonding (Kryachko and Remacle, 2005). However, $NH_2$ terminated group of DNA can form covalent immobilization with some functional groups such as carboxyl that exists in the polymers (Abdul Rashid and Yusof, 2017).

After fabrication of DNA/PMET-AuNPs/PGE and in the determination step, $Hg^{2+}$ is reduced preconcentrated on the electrode surface. Finally, the oxidation peak current was investigated using SWASV at 0.25 V.

### 3.2. The results of FESEM-EDS and AFM

Fig. 1 shows the field emission scanning electron microscopy (FE-SEM) images obtained to investigate the morphologies of the and modified PGEs. Fig. 1A presents the surface of PMET-AuNPs/PGE. As can be seen in Fig. 1A, AuNPs were established on the electrode surface. Most of AuNPs were dispersed on the electrodes surface in the FE-SEM image, exhibiting a large surface area. Moreover, Fig. 1B shows SEM of DNA/PMET-AuNPs/PGE surface. Energy dispersive X-ray spectroscopy (EDS) analysis was utilized to check the elements present in the modified electrodes. The EDS experiments showed that atomic percent of Au reached from zero at bare PGE to 0.88 at PMET-AuNPs/PGE and to 0.99 at DNA/PMET-AuNPs/PGE which it confirms deposition of Au. On the other hand, atomic percent of P from zero at bare PGE and PMET-AuNPs/PGE, increased to 0.2 at DNA/PMET-AuNPs/PGE which it is attributed to the presence of DNA (Nithiyanantham et al., 2014).

Atomic force microscopy (AFM) analysis was applied to investigate the surface morphology of the bare PGE, PMET-AuNPs/PGE, and DNA/PMET-AuNPs/PGE. Fig. S2 illustrates the two-dimensional (2D) and three-dimensional (3D) AFM images of the bare PGE, PMET-AuNPs/PGE, and DNA/PMET-AuNPs/PGE. As shown in Fig. S2A, in the bare PGE, a lumpy surface is seen. In comparison, Fig. S2B displays a smoother layer based on polymer formation. Fig. S2C illustrates surface morphology of DNA/PMET-AuNPs/PGE. The comparison of AFM images reveals a marked difference in the roughness of the surfaces bare PGE with DNA/PMET-AuNPs/PGE and PMET-AuNPs/PGE and similarity roughness between DNA/PMET-AuNPs/PGE and PMET-AuNPs/PGE. The roughness was obtained from AFM image as 139, 97 and 102 nm for bare PGE, PMET-AuNPs/PGE, and DNA/PMET-AuNPs/PGE electrodes, respectively. In other words, the bare PGE surface has a high amount of roughness but when the polymer layer of PMET-AuNPs is formed on the PGE surface and the DNA is immobilized on this polymeric surface, the roughness decreases. This roughness reduction can probably lead to a more compact and stable layer on the electrode surface.

### 3.3. Electrochemical impedance spectroscopy results

It is well known that electrochemical impedance spectroscopy (EIS) is an effective tool for studying the interface properties of surface-modified electrodes. The electrical conductivity is one of the most important properties of the modified electrode. In this study, impedance measurements were used for conductivity studies. Fig. 2A shows EIS results of the bare PGE, PMET-AuNPs/PGE, and DNA/PMET-AuNPs/PGE in the presence of 5.0 mM $K_3[Fe(CN)_6]/K_4[Fe(CN)_6]$ solution and 0.1 M KCl. It is therefore clear that the PMET-AuNPs/PGE can increase the electron transfer compared with bare PGE with respect to presence of conductive PMET and AuNPs. However, the presence of DNA has a lower effect on the conductivity rather than its absence. The equivalent circuit with the Nyquist diagram is shown in Fig. S3. In the circuit shown in Fig. S3A, $R_s$, $CPE_{dl,}$ and $R_{ct}$ represent solution resistance, a constant phase element corresponding to the double-layer capacitance, and the charge-transfer resistance, respectively. W is a finite-length Warburg impedance short-circuit term coupled to $R_{ct}$, which accounts for the Nernstian diffusion. In the circuit above, the charge transfer resistance of the electrode reaction is the only circuit element that has a simple physical meaning, illustrating how fast the charge transfer rate changes during the reaction of the modified and unmodified electrode with the electrode potential. The $R_{ct}$ values for bare PGE, PMET-AuNPs/PGE, and DNA/PMET-AuNPs/PGE were obtained at 958, 640, and 604 Ω, respectively using fitting obtained data in the above circuit (Fig. S3).

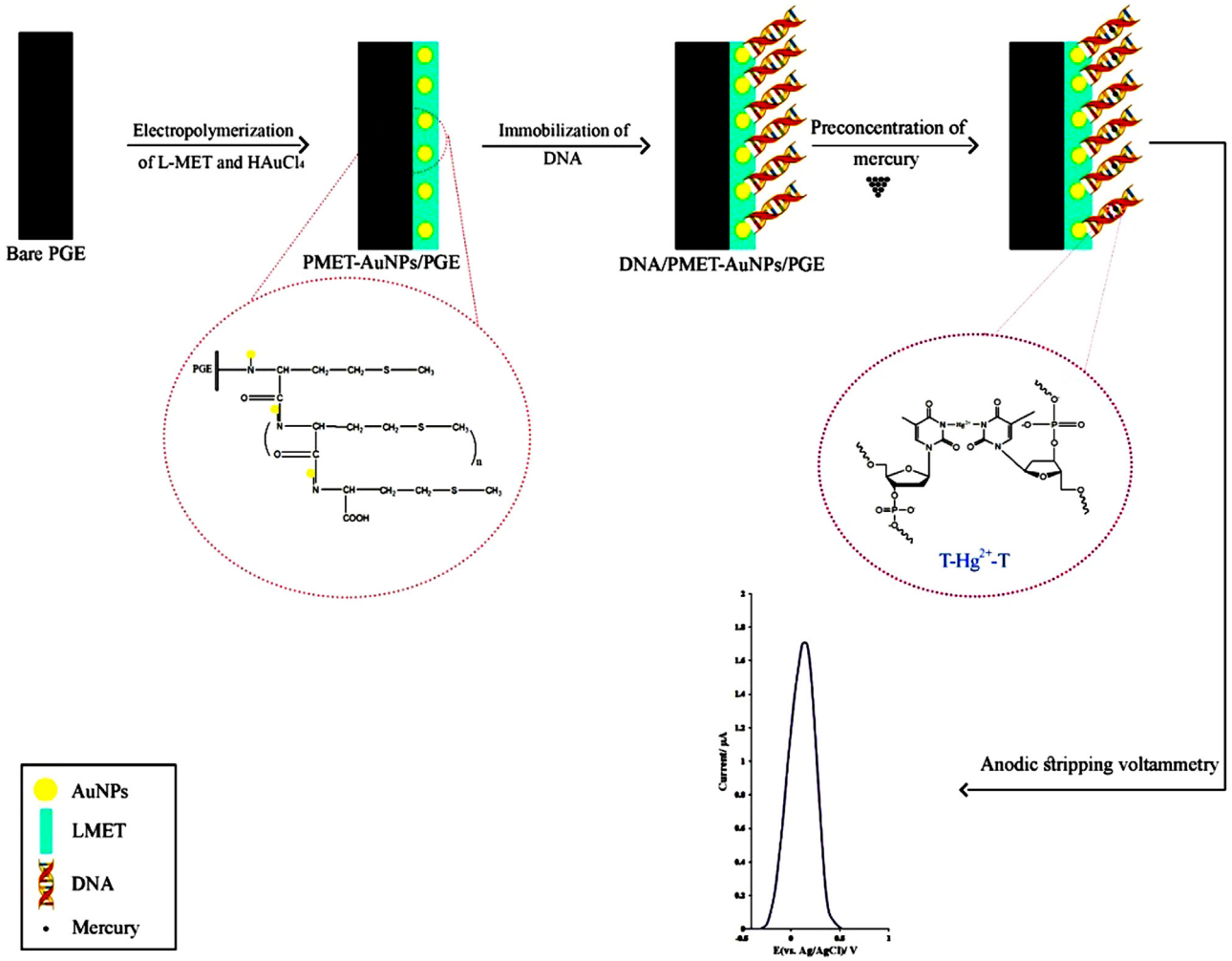


**Scheme 1.** A schematic of fabrication of the DNA/PMET-AuNPs/PGE electrochemical sensor for mercury(II) detection.

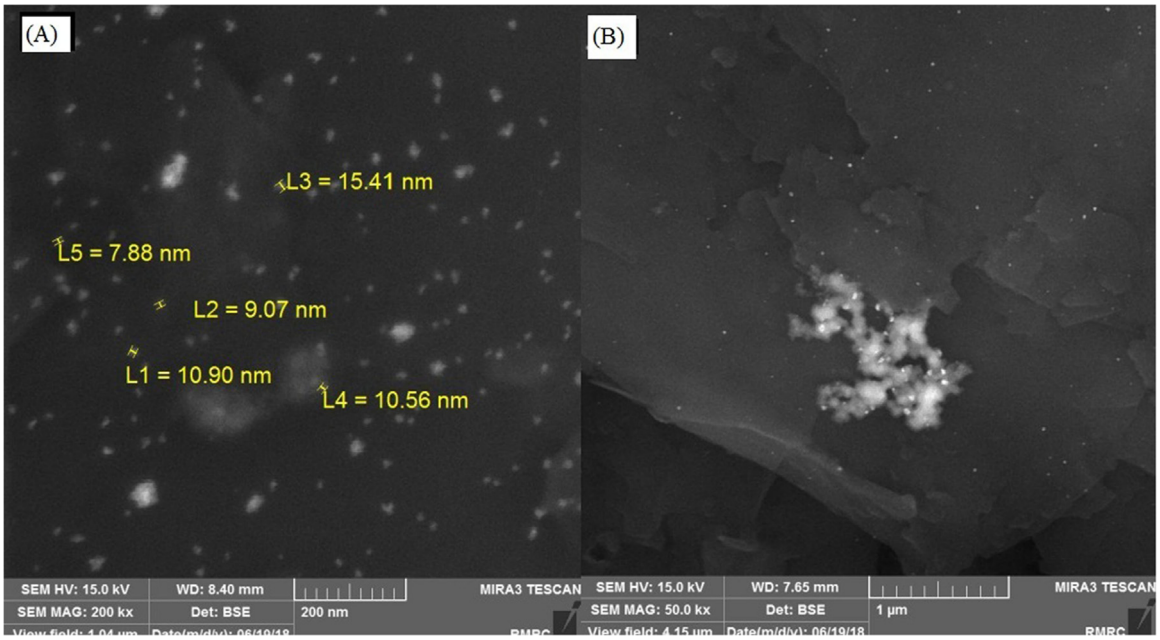


**Fig. 1.** FE-SEM images of (A) PMET-AuNPs/PGE and (B) DNA/PMET-AuNPs/PGE.

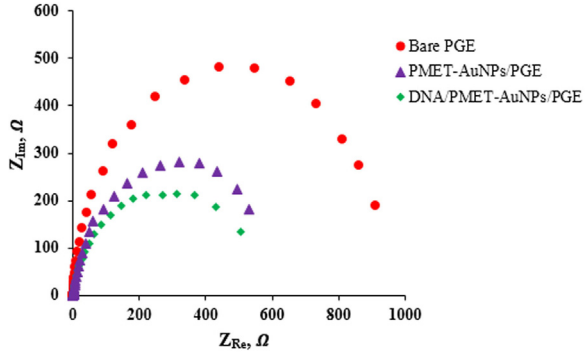


**Fig. 2.** (A) EIS of bare PGE, PMET-AuNPs/PGE, and DNA/PMET-AuNPs/PGE in the presence of 5.0 mM $K_3[Fe(CN)_6]/K_4[Fe(CN)_6]$ solution and 0.1 M KCl.

### 3.4. Electrochemical behavior of $Hg^{2+}$ at un-modified and the modified PGE electrodes

Fig. S4 shows the comparison of mercury(II) nitrate detection on the bare PGE, PMET-AuNPs/PGE and DNA/PMET-AuNPs/PGE using SWASV in 0.1 pM $Hg^{2+}$ solution and pH 3. SWASV curves responses were recorded in the positive potential range of -0.1 V to 0.6 V. Based on this figure, no observable signal was obtained on the bare electrode whereas, the signals increases with the progress in modification steps. In addition, the DNA/PMET-AuNPs /PGE shows a well-defined peak current that is 2.5 times higher than that of PMET-AuNPs/PGE. As can be seen, this electrode represents the highest signal compared to the others. In many of the heavy metal ion sensors, the target metal ion ($Hg^{2+}$) is adsorbed on the modified electrodes as metal form (Eq. (1)) during the period of pre-deposition treatment. As a result, it undergoes oxidation reaction (Eq. (1)) during the determination step. $Hg^{2+}$ can be adsorbed on the DNA/PMET-AuNPs /PGE regarding its high interaction with DNA and PMET (see in Supplementary material and Fig. S5). However, the presence of AuNPs amplifies the signal due to their high surface area and also high conductivity.

$$Hg^{2+} + 2e^- \rightarrow Hg^0 \quad (1)$$

$$Hg^0 \rightarrow Hg^{2+} + 2e^- \quad (2)$$

The effective surface area was also computed based on chronocoulometry experiments (see in Supplementary material and Fig. S6) as 0.0132, 0.129, and 0.141 $cm^2$ for bare PGE, PMET-AuNPs/PGE, and DNA/PMET-AuNPs/PGE electrodes, respectively. It should be mentioned that the effective surface area or active electrochemical surface area is where electron exchange takes place and it is different from the geometrical surface area, which is simply the sum of all the physical areas that cover the surface of the electrode (Fragkou et al., 2012). These results show the expansion of surface area with the progress in

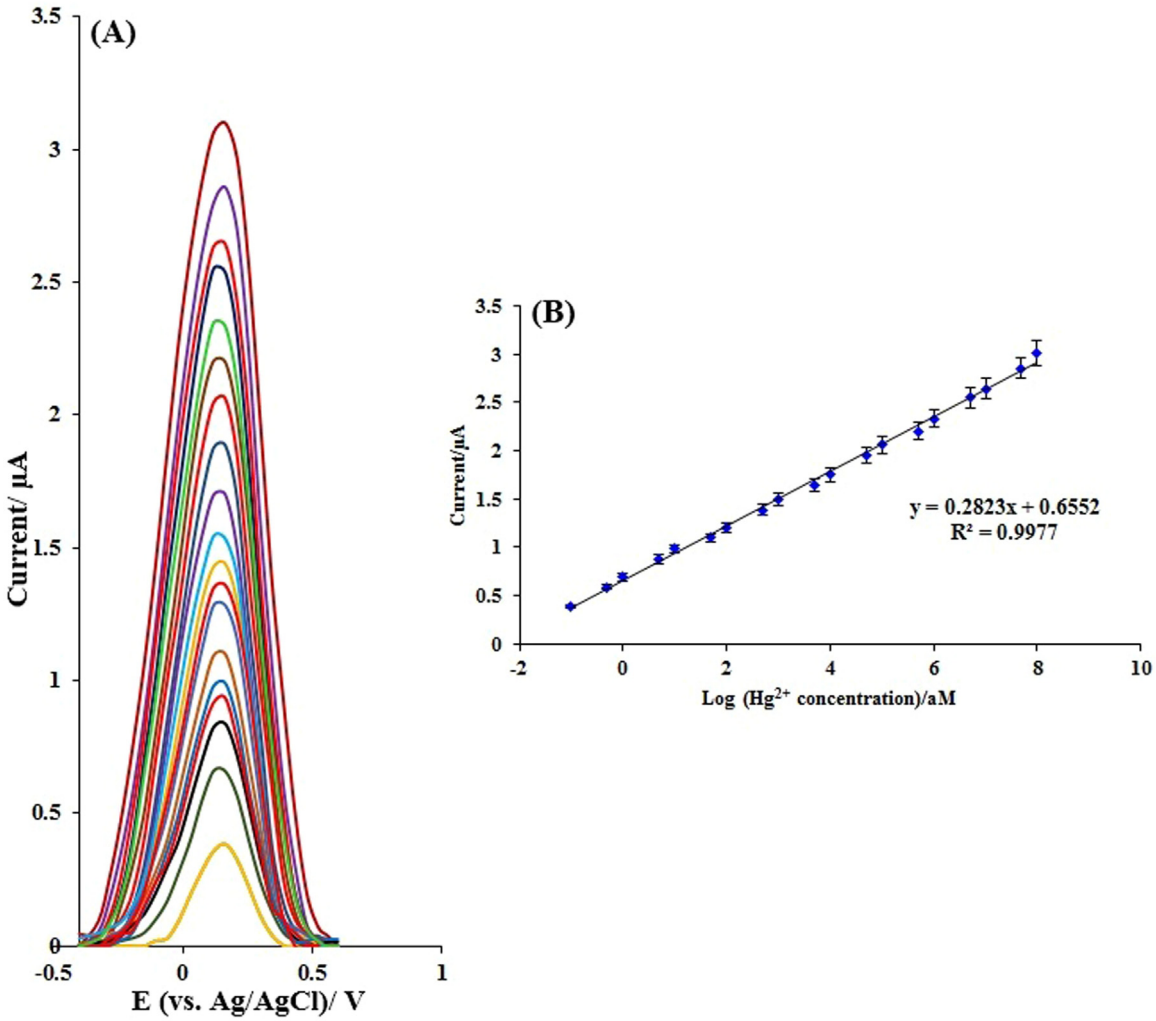


**Fig. 3.** (A) Square wave voltammograms of $Hg^{2+}$ at DNA/PMET-AuNPs/PGE in pH 3 at frequency of 20 Hz with a step potential of 5 mV, deposition potential 0 V and deposition time 250 s (containing different concentrations of $Hg^{2+}$ from 0.1 aM 0.1 nM) (B) the linear relationship between the current responses versus logarithm of concentration of $Hg^{2+}$.

the modification.

### 3.5. Optimization of experimental parameters

In order to maximize the efficiency of the DNA/PMET-AuNPs/PGE, some effective parameters on the fabrication of electrode and determination of $Hg^{2+}$ should be optimized. These parameters are included (I) concentration of L-MET, (II) concentration of $HAuCl_4$, (III) the number of cycles for polymerization of L-MET and entrapment of AuNPs, (IV) scan rate of the polymerization of L-MET-$HAuCl_4$, (V) concentration of DNA, (VI) immobilization potential of DNA, (VII) immobilization time of DNA, (VIII) effect of pH and effective parameters on the deposition of $Hg^{2+}$ such as (IX) deposition time, (X) deposition potential of $Hg^{2+}$, and also (XI) effect of frequency in SWV technique. The optimization these parameters are explained in the Supplementary material and Fig. S7.

### 3.6. The calibration curve, detection limit, reproducibility, and stability of DNA/PMET-AuNPs/PGE

SWASV was applied for the determination of $Hg^{2+}$ ion using the DNA/PMET-AuNPs/PGE and the obtained voltammograms are shown in Fig. 3A. Fig. 3B presents the linear correlation between peak current and the logarithm of $Hg^{2+}$ concentration at DNA/PMET-AuNPs/PGE in the range between 0.1 aM and 0.1 nM with a correlation coefficient of 0.9977.

The limit of detection (LOD) was determined as $3S_b/m$; where $S_b$ is the standard deviation of blank for five replica determinations and 'm' is the slope of the calibration curve. LOD for $Hg^{2+}$ with the DNA/PMET-AuNPs/PGE was 0.004 aM. We compared the results of this modified electrode with some other methods used for $Hg^{2+}$ detection and listed the results in Table 1. In brief, the novel DNA/PMET-AuNPs/PGE for the sensing of $Hg^{2+}$ shows a very low detection limit and wide linear dynamic range.

The reproducibility of the suggested modified electrode was examined to detect 30.0 aM $Hg^{2+}$ by SWASV method. The current response of $Hg^{2+}$ was determined by five different modified electrodes (Fig. S8). The relative standard deviation (RSD) for five measurements was obtained as 4.6%. The repeatability of DNA/PMET-AuNPs/PGE modified electrode was also investigated with five determinations of 30.0 aM $Hg^{2+}$ with one modified electrode. The RSD was calculated as 3.7%. In order to investigate the stability of the DNA/PMET-AuNPs/PGE electrode, the SWASV current responses for 30.0 aM $Hg^{2+}$ in pH 3.0 was recorded over a period of 30 days. The response was reduced to 90% principal response after 3 days and to 80% after 12 days and after that, it was nearly constant to 30 days (Fig. S9). Also, to investigate stability of electrode composition in pH 3, the modified electrode was placed in solution with pH 3 and then the SWASV current responses for 500 nM $Hg^{2+}$ were measured. As, Fig. S10 shows the response does not change over a period 60 min.

### 3.7. Interferences study

To assay selectivity of the DNA/PMET-AuNPs/PGE, various possible interfering species were investigated for their possible effects on the determination of $Hg^{2+}$. The experimental results were compared with that for 0.01 nM $Hg^{2+}$ detection. The results showed that a 10.0 nM increase in $In^{3+}$, $Ge^{4+}$, $V^{4+}$, $Mg^{2+}$, $Pb^{2+}$, $Cd^{2+}$, $Zn^{2+}$, $Ca^{2+}$ and $Fe^{3+}$, and a 1.0 nM increase in $Sn^{2+}$, $Cr^{3+}$, $Cu^{2+}$ and $Ag^{+}$ have no interference on the determination of 0.01 nM $Hg^{2+}$ using DNA/PMET-AuNPs/PGE. The results show more selectivity of the sensor for $Hg^{2+}$ compared to the others. The high selectivity of the sensor is related to the specific coordination between $Hg^{2+}$ and T bases of DNA, which can lead to the formation of stable complex T-$Hg^{2+}$-T. On the other hand, in addition to the more sensitivity of fabricated biosensor to $Hg^{2+}$ compared with some other metal ions such as $Pb^{2+}$, $Cd^{2+}$, and $Cu^{2+}$ (that are seen commonly in the real samples), the responses of these ions are seen at different potentials and also application of deposition potential 0 V in the preconcentration step, helps to increase the selectivity of method. Since metal ions with more negative standard potentials, cannot reduce in this potential. Therefore, the fabricated biosensor shows a good selective response to $Hg^{2+}$ against other metal ions.

### 3.8. Application of DNA/PMET-AuNPs/PGE in the analysis of environmental samples

The practical application of the DNA/PMET-AuNPs/PGE electrochemical biosensor was studied for determination of $Hg^{2+}$ in real samples such as sea water and the fish samples. The SWASV technique was employed for $Hg^{2+}$ determination in real samples based on the optimal parameters of the suggested method. For this purpose, initially, the sea water and the fish samples, which were prepared in according to the Experimental section, were spiked with different concentrations of $Hg^{2+}$ and then the proposed method was applied to determine their $Hg^{2+}$ amounts using standard addition method. The determination

**Table 1**
Detection limit and linear dynamic range of various electrochemical methods for determination of $Hg^{2+}$.

| Electrode | Method | Linear dynamic range | Detection limit | References |
|---|---|---|---|---|
| Functionalized gold nanoparticles/reduced graphene oxide | DPV[a] | 10 ng $L^{-1}$ to 1.0 μg $L^{-1}$ | 1.5 ng $L^{-1}$ | (N. Wang et al., 2016) |
| Gold nanoparticle-bioconjugate and thymine–$Hg^{2+}$–thymine | DPV | 0.05–2.5 nM | 7.38 pM | (Tang et al., 2012) |
| Target-induced structure-switching DNA | DPV | 0.1 nM to 5.0 μM | 0.06 nM | (Wu et al., 2010) |
| DNA/Graphen-Au | SWV | 1.0 aM to 100 nM | 0.001 aM | (Zhang et al., 2015) |
| EDTA/CPE[b] | SWV | $5 \times 10^{-5}$ to $35 \times 10^{-5}$ M | $16.6 \times 10^{-9}$ M | (Moutcine and Chtaini, 2018) |
| AV-HA/GCE[c] | SWV | $2 \times 10^{-7}$ to $2.1 \times 10^{-4}$ M | 141 nM | (Kanchana et al., 2015) |
| $PPh_3$/MWCNTs/IL/CPE[d] | SWASV | $1 \times 10^{-4}$ to 0.15 μM | $9.2 \times 10^{-5}$ μM | (Bagheri et al., 2013) |
| Au/DMAET/(SWCNT-PABS)[e] | SWASV | 20–250 μM | 0.06 μM | (Matlou et al., 2016) |
| AuNPs/CFME[f] | DPASV | 0.2–50 μM | 0.1 μM | (Li et al., 2014) |
| Np- AuNPs/ITO[g] | DPASV[h] | 0.1–10 μM | 0.03 μM | (Lin et al., 2015) |
| DNA/PMET-AuNPs/PGE | SWASV | 0.1 aM to 0.1 nM | 0.004 aM | This work |

[a] Differential pulse voltammetry (DPV).
[b] Ethylene diamine tetra acetic acid (EDTA)/ carbon paste electrode.
[c] Aloe vera- hydroxyapatite/ glassy carbon electrode.
[d] Triphenyl phosphine/ multiwalled carbon nanotube/ ionic liquid/ carbon paste electrode.
[e] Au/ 2-dimethyl amino ethane thiol hydrochloride/ (single walled carbon nanotube-poly (m-amino benzene sulfonic acid)).
[f] Gold nanoparticles decorated carbon fiber electrode.
[g] Nanoporous gold nanoparticles/indium tin oxide electrode.
[h] Differential pulse anodic stripping voltammetry.

**Table 2**
Determination of $Hg^{2+}$ in environmental samples.

| Sample | Add (pM) | Found (pM) | % Recovery |
|---|---|---|---|
| Sea water[a] | 0.0 | 1.4 ± 0.1[c] | – |
| | 3.0 | 4.1 ± 0.2 | 90.0 |
| | 5.0 | 6.7 ± 0.2 | 106.0 |
| Fish[b] | 0.0 | 1.0 ± 0.1 | – |
| | 3.0 | 3.9 ± 0.2 | 96.6 |
| | 5.0 | 6.6 ± 0.3 | 112.0 |

[a] Caspian sea.
[b] Caspian white fish.
[c] Mean ± standard deviation (for triplicate determinations).

results (Table 2) show that the recovery percentage was in the range of 90.0–106.0% and 96.6–112.0% for sea water and fish samples, respectively.

## 4. Conclusions

In this paper, DNA/PMET-AuNPs/PGE was simply fabricated by electropolymerization of L-MET and electrochemical entrapment of AuNPs and eventually immobilization of DNA on the PMET-AuNPs/PGE. This sensor showed excellent performance toward $Hg^{2+}$ determination such as very low detection limit, wide linear dynamic range and suitable selectivity. Two components of the sensor contribute to its significant improvement of detection performance: 1) PMET-AuNPs were conveniently electrodeposited onto the electrode surface for improving electrode performance. In addition to enhancing effects of AuNPs and poly-L-methionine, the presence of them on the sensor surface provides a suitable platform for immobilization of DNA because of coordination interaction between DNA bases and AuNPs and also the presence of carboxyl groups in poly-L-methionine. 2) The strategy employed in this study mainly deals with the determination of $Hg^{2+}$ based on specific combination between $Hg^{2+}$ and DNA (especially T bases of DNA to form stable T-$Hg^{2+}$-T linkage). The fabricated sensor can be developed for detection of $Hg^{2+}$ in different real samples and also for simultaneous determination of some heavy metals using chemometrics methods in the future. However, the species with very near oxidation potential to Hg and also very high interaction with DNA may be interfered in the determination of $Hg^{2+}$ using this method.

## Acknowledgements

The authors acknowledge the Research Council of Damghan University for partial support of this work.

## Appendix A. Supporting information

Supplementary data associated with this article can be found in the online version at https://doi.org/10.1016/j.bios.2018.12.039.

## References

Abdul Rashid, J.I., Yusof, N.A., 2017. The strategies of DNA immobilization and hybridization detection mechanism in the construction of electrochemical DNA sensor: a review. Sens. BioSens. Res. 16, 19–31.
Anastassopoulou, J., 2003. Metal–DNA interactions. J. Mol. Struct. 651–653, 19–26.
Aragay, G., Merkoçi, A., 2012. Nanomaterials application in electrochemical detection of heavy metals. Electrochim. Acta 84, 49–61.
Azadmehr, F., Zarei, K., 2018. Ultrasensitive determination of ceftizoxime using pencil graphite electrode modified by hollow gold nanoparticles/reduced graphene oxide. Arab. J. Chem. https://doi.org/10.1016/j.arabjc.2018.02.004. (in press).
Bagheri, H., Afkhami, A., Khoshsafar, H., Rezaei, M., Shirzadmehr, A., 2013. Simultaneous electrochemical determination of heavy metals using a triphenylphosphine/MWCNTs composite carbon ionic liquid electrode. Sens. Actuators B 186, 451–460.
Bernalte, E., Sánchez, C.M., Gil, E.P., 2012. Determination of Mercury in indoor dust samples by ultrasonic probe microextraction and stripping voltammetry on gold nanoparticles-modified screen-printed electrodes. Talanta 97, 187–192.
Bojdi, M.K., Behbahani, M., Omidi, F., Hesam, G., 2016. Application of a novel electrochemical sensor based on modified siliceous mesocellular foam for electrochemical detection of ultra-trace amounts of mercury ions. New J. Chem. 40, 4519–4527.
Cui, L., Wu, J., Ju, H., 2015. Electrochemical sensing of heavy metal ions with inorganic, organic and bio-materials. Biosens. Bioelectron. 63, 276–286.
Duffus, J.H., Worth, H.G.J., 2006. Fundamental Toxicology. Royal Society of Chemistry, Cambridge.
Fragkou, V., Ge, Y., Steiner, G., Freeman, D., Bartetzko, N., Turner, A.P.F., 2012. Determination of the real surface area of a screen-printed electrode by chronocoulometry. Int. J. Electrochem. Sci. 7, 6214–6220.
Ghaedi, M., Ahmadi, F., Shokrollahi, A., 2007. Simultaneous preconcentration and determination of copper, nickel, cobalt and lead ions content by flame atomic absorption spectrometry. J. Hazard. Mater. 142, 272–278.
Gómez-Ariza, J.L., Lorenzo, F., García-Barrera, T., 2005. Comparative study of atomic fluorescence spectroscopy and inductively coupled plasma mass spectrometry for mercury and arsenic multispeciation. Anal. Bioanal. Chem. 382, 485–492.
Kanchana, P., Sudhan, N., Anandhakumar, S., Mathiyarasu, J., Manisankar, P., Sekar, C., 2015. Electrochemical detection of mercury using biosynthesized hydroxyapatite nanoparticles modified glassy carbon electrodes without preconcentration. RSC Adv. 5, 68587–68594.
Kryachko, E.S., Remacle, F., 2005. Complexes of DNA bases and Watson-Crick base pairs with small neutral gold clusters. J. Phys. Chem. B 109, 22746–22757.
Li, D., Li, J., Jia, X., Wang, E., 2014. Gold nanoparticles decorated carbon fiber mat as a novel sensing platform for sensitive detection of Hg (II). Electrochem. Commun. 42, 30–33.
Lin, Y., Peng, Y., Di, J., 2015. Electrochemical detection of Hg (II) ions based on nanoporous gold nanoparticles modified indium tin oxide electrode. Sens. Actuators B 220, 1086–1090.
Locatelli, C., Melucci, D., 2013. Voltammetric method for ultra-trace determination of total mercury and toxic metals in vegetables. Comparison with spectroscopy. Open Chem. 11, 790–800.
Matlou, G.G., Nkosi, D., Pillay, K., Arotiba, O., 2016. Electrochemical detection of Hg (II) in water using self-assembled single walled carbon nanotube-poly (m-amino benzene sulfonic acid) on gold electrode. Sens. Biosens. Res. 10, 27–33.
Moutcine, A., Chtaini, A., 2018. Electrochemical determination of trace mercury in water sample using EDTA-CPE modified electrode. Sens. Biosens. Res. 17, 30–35.
Nejdl, L., Ruttkay-Nedecky, B., Kudr, J., Kremplova, M., Cernei, N., Prasek, J., Konecna, M., Hubalek, J., Zitka, O., Kynicky, J., 2013. Behaviour of zinc complexes and zinc sulphide nanoparticles revealed by using screen printed electrodes and spectrometry. Sensors 13, 14417–14437.
Nejdl, U., Kudr, J., Cihalova, K., Chudobova, D., Zurek, M., Zalud, L., Kopecny, L., Burian, F., Ruttkay–Nedecky, B., Krizkova, S., 2014. Remote-controlled robotic platform ORPHEUS as a new tool for detection of bacteria in the environment. Electrophoresis 35, 2333–2345.
Nithiyanantham, U., Ramadoss, A., Rao Ede, S., Kundu, S., 2014. DNA mediated wire-like clusters of self-assembled TiO2 nanomaterials: supercapacitor and dye sensitized solar cell applications. Nanoscale 6, 8010–8023.
Nourifard, F., Payehghadr, M., Kalhor, M., Nejadali, A., 2015. An electrochemical sensor for determination of Ultratrace Cd, Cu and Hg in water samples by modified carbon paste electrode base on a new Schiff base ligand. Electroanalysis 27, 2479–2485.
Nowka, R., Marr, I.L., Ansari, T.M., Müller, H., 1999. Direct analysis of solid samples by GFAAS–determination of trace heavy metals in barytes. Fresenius J. Anal. Chem. 364, 533–540.
Ojani, R., Alinezhad, A., Abedi, Z., 2013. A highly sensitive electrochemical sensor for simultaneous detection of uric acid, xanthine and hypoxanthine based on poly (L-methionine) modified glassy carbon electrode. Sens. Actuators B 188, 621–630.
Rafiee, B., Fakhari, A.R., Ghaffarzadeh, M., 2015. Impedimetric and stripping voltammetric determination of methamphetamine at gold nanoparticles-multiwalled carbon nanotubes modified screen printed electrode. Sens. Actuators B 218, 271–279.
Ramesh, G.V., Radhakrishnan, T.P., 2011. A universal sensor for mercury (Hg, HgI, HgII) based on silver nanoparticle-embedded polymer thin film. ACS Appl. Mater. Interfaces 3, 988–994.
Reza Ojani, J.-B.R., Maleki, Ali Asghar, Safshekan, Saeid, 2014. Simultaneous and sensitive detection of dopamine and uric acid using a poly(L-methionine)/gold nanoparticle-modified glassy carbon electrode. Chin. J. Catal. 35, 423–429.
Rezaei, B., Boroujeni, M., Ensafi, A.A., 2015. Fabrication of DNA, o-phenylenediamine, and gold nanoparticle bioimprinted polymer electrochemical sensor for the determination of dopamine. Biosens. Bioelectron. 66, 490–496.
Shirzadmehr, A., Afkhami, A., Madrakian, T., 2015. A new nano-composite potentiometric sensor containing an Hg2+-ion imprinted polymer for the trace determination of mercury ions in different matrices. J. Mol. Liq. 204, 227–235.
Tang, X., Liu, H., Zou, B., Tian, D., Huang, H., 2012. A fishnet electrochemical Hg2+ sensing strategy based on gold nanoparticle-bioconjugate and thymine–$Hg^{2+}$–thymine coordination chemistry. Analyst 137, 309–311.
Venkataprasad, G., Reddy, T.M., Shaikshavali, P., Gopal, P., 2018. A novel electrochemical sensor based on multi-walled carbon nanotubes/poly (L-Methionine) for the investigation of 5-nitroindazole: a voltammetric study. Anal. Chem. Lett. 8, 457–474.
Wang, H., Zhang, Y., Ma, H., Ren, X., Wang, Y., Zhang, Y., Wei, Q., 2016. Electrochemical DNA probe for Hg2+ detection based on a triple-helix DNA and multistage signal amplification strategy. Biosens. Bioelectron. 86, 907–912.
Wang, N., Lin, M., Dai, H., Ma, H., 2016. Functionalized goldnanoparticles/reducedgrapheneoxide nanocomposites for ultrasensitive electrochemical sensing of mercury ions based on thymine–mercury–thymine structure. Biosens. Bioelectron. 79, 320–326.
Wu, D., Zhang, Q., Chu, X., Wang, H., Shen, G., Yu, R., 2010. Ultrasensitive electrochemical sensor for mercury (II) based on target-induced structure-switching DNA.

Biosens. Bioelectron. 25, 1025–1031.
Yin, C., Iqbal, J., Hu, H., Liu, B., Zhang, L., Zhu, B., Du, Y., 2012. Sensitive determination of trace mercury by UV–visible diffuse reflectance spectroscopy after complexation and membrane filtration-enrichment. J. Hazard. Mater. 233, 207–212.
Zarei, K., Khodadadi, A., 2017. Very sensitive electrochemical determination of diuron on glassy carbon electrode modified with reduced graphene oxide-gold nanoparticle-Nafion composite film. Ecotoxicol. Environ. Saf. 144, 171–177.
Zhang, B., Guo, I.H., 2012. Highly sensitive and selective photoelectrochemical DNA sensor for the detection of $Hg^{2+}$ in aqueous solutions. Biosens. Bioelectron. 37, 112–115.
Zhang, F., Gu, S., Ding, Y., Zhou, L., Zhang, Z., Li, L., 2013. Electrooxidation and determination of cefotaxime on Au nanoparticles/poly (L-arginine) modified carbon paste electrode. J. Electroanal. Chem. 698, 25–30.
Zhang, Y., Zeng, G.M., Tang, L., Chen, J., Zhu, Y., He, X.X., He, Y., 2015. Electrochemical sensor based on electrodeposited graphene-Au modified electrode and nanoAu carrier amplified signal strategy for attomolar mercury detection. Anal. Chem. 87, 989–996.
Zhu, C., Yang, G., Li, H., Du, D., Lin, Y., 2014. Electrochemical sensors and biosensors based on nanomaterials and nanostructures. Anal. Chem. 87, 230–249.
Zhu, X., Alexandratos, S.D., 2007. Determination of trace levels of mercury in aqueous solutions by inductively coupled plasma atomic emission spectrometry: elimination of the 'memory effect'. Microchem. J. 86, 37–41.
Zuo, X., Wu, H., Toh, J., Li, S.F.Y., 2010. Mechanism of mercury detection based on interaction of single-strand DNA and hybridized DNA with gold nanoparticles. Talanta 82, 1642–1646.